



ANTARES constrains a blazar origin of two IceCube PeV neutrino events

S. Adrián-Martínez, A. Albert, M. André, G. Anton, M. Ardid, J.-J. Aubert, B. Baret, J. Barrios, S. Basa, V. Bertin, et al.

► To cite this version:

S. Adrián-Martínez, A. Albert, M. André, G. Anton, M. Ardid, et al.. ANTARES constrains a blazar origin of two IceCube PeV neutrino events. *Astronomy and Astrophysics - A&A*, 2015, 576, pp.L8. 10.1051/0004-6361/201525670 . cea-01300542

HAL Id: cea-01300542

<https://cea.hal.science/cea-01300542>

Submitted on 11 Apr 2016

HAL is a multi-disciplinary open access archive for the deposit and dissemination of scientific research documents, whether they are published or not. The documents may come from teaching and research institutions in France or abroad, or from public or private research centers.

L'archive ouverte pluridisciplinaire **HAL**, est destinée au dépôt et à la diffusion de documents scientifiques de niveau recherche, publiés ou non, émanant des établissements d'enseignement et de recherche français ou étrangers, des laboratoires publics ou privés.

LETTER TO THE EDITOR

ANTARES constrains a blazar origin of two IceCube PeV neutrino events[★]

The ANTARES Collaboration: S. Adrián-Martínez¹, A. Albert², M. André³, G. Anton⁵, M. Ardid¹, J.-J. Aubert⁶, B. Baret⁷, J. Barrios⁸, S. Basa⁹, V. Bertin⁶, S. Biagi²⁴, C. Bogazzi¹², R. Bormuth^{12,13}, M. Bou-Cabo¹, M. C. Bouwhuis¹², R. Bruijn^{12,14}, J. Brunner⁶, J. Bustó⁶, A. Capone^{15,16}, L. Caramete¹⁷, J. Carr⁶, T. Chiarusi¹⁰, M. Circella¹⁸, R. Coniglione²⁴, H. Costantini⁶, P. Coyle⁶, A. Creusot⁷, G. De Rosa^{19,20}, I. Dekeyser^{21,22}, A. Deschamps²³, G. De Bonis^{15,16}, C. Distefano²⁴, C. Donzaud^{7,25}, D. Dornic⁶, Q. Dorosti²⁶, D. Drouhin², A. Dumas²⁷, T. Eberl⁵, A. Enzenhöfer⁵, S. Escoffier⁶, K. Fehn⁵, I. Felis¹, P. Fermani^{15,16}, F. Folger⁵, L. A. Fusco^{10,11}, S. Galatà⁷, P. Gay²⁷, S. Geißelsöder⁵, K. Geyer⁵, V. Giordano²⁸, A. Gleixner⁵, J. P. Gómez-González⁸, R. Gracia-Ruiz⁷, K. Graf⁵, H. van Haren²⁹, A. J. Heijboer¹², Y. Hello²³, J. J. Hernández-Rey⁸, A. Herrero¹, J. Hößl⁵, J. Hofestädt⁵, C. Hugon^{4,36}, C. W James^{5,**}, M. de Jong^{12,13}, O. Kalekin⁵, U. Katz⁵, D. Kießling⁵, P. Kooijman^{12,14,30}, A. Kouchner⁷, V. Kulikovskiy²⁴, R. Lahmann⁵, D. Lattuada²⁴, D. Lefèvre^{21,22}, E. Leonora^{28,32}, H. Loehner²⁶, S. Loucas³³, S. Mangano⁸, M. Marcellin⁹, A. Margiotta^{10,11}, J. A. Martínez-Mora¹, S. Martini^{21,22}, A. Mathieu⁶, T. Michael¹², P. Migliozzi¹⁹, M. Neff⁵, E. Nezri⁹, D. Palioselitis¹², G. E. Páválaš¹⁷, C. Perrina^{15,16}, P. Piattelli²⁴, V. Popa¹⁷, T. Pradier³⁴, C. Racca², G. Riccobene²⁴, R. Richter⁵, K. Roensch⁵, A. Rostovtsev³⁵, M. Saldaña¹, D. F. E. Samtleben^{12,13}, A. Sánchez-Losa⁸, M. Sanguineti^{4,36}, P. Sapienza²⁴, J. Schmid⁵, J. Schnabel⁵, S. Schulte¹², F. Schüssler³³, T. Seitz⁵, C. Sieger⁵, A. Spies⁵, M. Spurio^{10,11}, J. J. M. Steijger¹², Th. Stolarczyk³³, M. Taiuti^{4,36}, C. Tamburini^{21,22}, Y. Tayalati³⁷, A. Trovato²⁴, M. Tselengidou⁵, C. Tönnis⁸, B. Vallage⁶, V. Van Elewyck⁷, E. Visser¹², D. Vivolo^{19,20}, S. Wagner⁵, E. de Wolf^{12,14}, H. Yepes⁸, J. D. Zornoza⁸, J. Zúñiga⁸, The TANAMI Collaboration: F. Krauß^{31,38}, M. Kadler^{38,**}, K. Mannheim³⁸, R. Schulz^{31,38}, J. Trüstede^{31,38}, J. Wilms³¹, R. Ojha^{39,40,41}, E. Ros^{42,43,44}, W. Baumgartner³⁹, T. Beuchert^{31,38}, J. Blanchard⁴⁵, C. Bürkel^{31,38}, B. Carpenter⁴¹, P. G. Edwards⁴⁶, D. Eisenacher Glawion³⁸, D. Elsässer³⁸, U. Fritsch⁵, N. Gehrels³⁹, C. Gräfe^{31,38}, C. Großberger⁴⁷, H. Hase⁴⁸, S. Horiuchi⁴⁹, A. Kappes³⁸, A. Kreikenbohm^{31,38}, I. Kreykenbohm³¹, M. Langejahn^{31,38}, K. Leiter^{31,38}, E. Litzinger^{31,38}, J. E. J. Lovell⁵⁰, C. Müller^{31,38}, C. Phillips⁴⁶, C. Plötz⁴⁸, J. Quick⁵¹, T. Steinbring^{31,38}, J. Stevens⁴⁶, D. J. Thompson³⁹, and A. K. Tzioumis⁴⁶

(Affiliations can be found after the references)

Received 15 January 2015 / Accepted 23 February 2015

ABSTRACT

Context. The source(s) of the neutrino excess reported by the IceCube Collaboration is unknown. The TANAMI Collaboration recently reported on the multiwavelength emission of six bright, variable blazars which are positionally coincident with two of the most energetic IceCube events. Objects like these are prime candidates to be the source of the highest-energy cosmic rays, and thus of associated neutrino emission.

Aims. We present an analysis of neutrino emission from the six blazars using observations with the ANTARES neutrino telescope.

Methods. The standard methods of the ANTARES candidate list search are applied to six years of data to search for an excess of muons – and hence their neutrino progenitors – from the directions of the six blazars described by the TANAMI Collaboration, and which are possibly associated with two IceCube events. Monte Carlo simulations of the detector response to both signal and background particle fluxes are used to estimate the sensitivity of this analysis for different possible source neutrino spectra. A maximum-likelihood approach, using the reconstructed energies and arrival directions of through-going muons, is used to identify events with properties consistent with a blazar origin.

Results. Both blazars predicted to be the most neutrino-bright in the TANAMI sample (1653–329 and 1714–336) have a signal flux fitted by the likelihood analysis corresponding to approximately one event. This observation is consistent with the blazar-origin hypothesis of the IceCube event IC 14 for a broad range of blazar spectra, although an atmospheric origin cannot be excluded. No ANTARES events are observed from any of the other four blazars, including the three associated with IceCube event IC20. This excludes at a 90% confidence level the possibility that this event was produced by these blazars unless the neutrino spectrum is flatter than –2.4.

Key words. neutrinos – galaxies: active – quasars: general

* Figures 2, 3 and Appendix A are available in electronic form at <http://www.aanda.org>

** Corresponding authors: C. W James, e-mail: clancy.james@physik.uni-erlangen.de; M. Kadler, e-mail: kadler@physik.uni-wuerzburg.de

1. Introduction

Since the initial report of the observation of two high-energy (\sim PeV) neutrino-induced cascades by the IceCube Collaboration (Aartsen et al. 2013), further observations using the high-energy starting-event (HESE) analysis have revealed an excess of events consistent with an isotropic, flavour-uniform flux of astrophysical neutrinos (IceCube Collaboration 2013; Aartsen et al. 2015, 2014). The small number of excess events (37 total, with an estimated background of 15), and directional resolution of typically 10° or worse for cascades, makes it difficult to resolve potential features of this flux, such as a spectral downturn above PeV energies, a steeper spectral index, and/or a contribution from one or more point-like sources of neutrinos. Consequently, many suggestions for the nature and origin(s) of this flux have been put forward. Of particular note is the suggestion of a point-source near the Galactic Centre producing the observed excess in that region (Razzaque 2013), a hypothesis already constrained by the ANTARES Collaboration (Adrián-Martínez et al. 2014a).

The TANAMI Collaboration has recently reported observations of six bright, variable blazars in positional coincidence with the range of possible arrival directions of the two PeV IceCube events IC 14 and IC 20 (Krauß et al. 2014)¹. Using a simple calculation based on the observed 1 keV to 10 GeV photon flux, the authors estimate that 1.9 ± 0.4 electron neutrino events at PeV energies would be expected in 662 days of IceCube data. This estimate compares well with the two observed events IC 14 and IC 20. Even taking this only as an order-of-magnitude indication of the expected event rate, a higher-resolution follow-up study of these objects is of great interest. Here, we present such an analysis using six years of data from the ANTARES neutrino telescope.

2. Target blazars and possible neutrino fluxes

The six blazars associated with the IC 14 and IC 20 fields by Krauß et al. (2014) are listed in Table 1. All exhibit prominent high-energy photon emission, and all but one are classified as flat-spectrum radio quasars (FSRQs; Véron-Cetty & Véron 2006). The predictions of the expected number of detected electron neutrino events were made by assuming a neutrino energy $E_\nu = 1$ PeV and a flavour-uniform flux, with total energy flux equal to that in high-energy photons. Active galactic nuclei (AGN) of all classes have long been proposed as sites of hadronic interaction, and are potential sources of the highest-energy cosmic rays and, hence, neutrinos (Berezinskii & Smirnov 1975; Hillas 1984; Stecker & Salamon 1996; Padovani & Resconi 2014). Predictions for the neutrino flux depend on the nature of the AGN considered, the cosmic-ray composition and flux, and the assumed densities of target hadronic matter and magnetic and photon fields (Szabo & Protheroe 1994; Mannheim 1995; Waxman & Bahcall 1999; Atoyan & Dermer 2001; Kelner et al. 2006; Becker Tjus et al. 2014; Dermer et al. 2014).

The emphasis on the two PeV events (IC 14 and IC 20; see Aartsen et al. 2014, for a full list) comes from the fact that these two highest-energy events have only a negligible probability for an atmospheric origin. While IC 14 and IC 20 are assumed to be ν_e charged-current (CC) events, and the most common production mechanism (photo-pion production) produces

a flux which is almost uniform in neutrino flavour at Earth, a flavour-dependent flux is predicted by different initial neutrino production mechanisms (Kistler et al. 2014; Anchordoqui 2015), and/or by invoking new physics during propagation (Beacom et al. 2003, and references therein).

The IceCube observations allow for the possibility of a sub-PeV flux of neutrinos from the sample blazars, in that four other events are positionally associated with the blazar sample (see Table 1). This is also consistent with the prediction of two ν_e charged-current (CC) events, since the low flavour-dependence of the IceCube HESE effective area at the highest energies means an equal number of ν_μ and ν_τ events would be expected from a flavour-uniform flux, but with a lower deposited energy. IceCube data are currently compatible with a flavour-uniform flux above 35 TeV (IceCube Collaboration et al. 2015), but a significant excess or deficit of track-like (mostly ν_μ CC) events in the cosmic diffuse flux cannot be excluded. Thus while these additional four events do not represent a significant excess above a diffuse background, the possibility that they may originate from the blazars in question should also be tested.

3. ANTARES candidate list search and expected sensitivity

ANTARES is an underwater neutrino telescope located in the Mediterranean Sea off the coast of Toulon, at $42^\circ 48' N, 6^\circ 10' E$ (Ageron et al. 2011). Consisting of an array of photomultiplier tubes, it is designed to record the induced Cherenkov light from the passage of energetic charged particles to infer the interactions of neutrinos.

The ANTARES candidate list search (CLS) methodology is described in Adrián-Martínez et al. (2012), with the latest results using six years of data (1338 days effective livetime) presented in Adrián-Martínez et al. (2014a). The search uses only up-going muons (i.e., those originating from below the horizon), with cuts placed on the fit quality of the muon track reconstruction and the estimated angular error. The long range of relativistic muons in seawater and the Earth's crust extends the effective detection volume to well beyond the physical size of the detector, in contrast with a HESE-like analysis. The six-year sample consists of 5516 events, with an estimated atmospheric muon contamination of 10%, and an estimated median angular resolution of 0.38° . A maximum-likelihood method is then used to estimate the relative contributions of signal and background fluxes, based on both the reconstructed event arrival directions and the fitted number of photon hits (a robust proxy for energy). We note that this method results in a non-integer number of signal events N_{sig} being estimated, since the signal and background fluxes maximising the likelihood of a given observation can take any normalisation. We also note that it is optimised assuming an E_ν^{-2} source spectrum, and it is sensitive almost exclusively to muon neutrinos. The ability of the ANTARES CLS to constrain the origin of the IceCube events is therefore dependent on the flavour ratio, which may vary according to the neutrino-production scenarios discussed in Sect. 2. Hereafter, sensitivities and limits will be shown for a uniform flavour ratio, from which results for non-uniform flavour fluxes can readily be derived.

The ability of the ANTARES CLS to probe the PeV-neutrino blazar-origin hypotheses of Krauß et al. (2014) can be seen from Fig. 1, which compares the time-integrated, flavour-averaged exposures of the ANTARES CLS (Adrián-Martínez et al. 2014a; 1338 days, using one third of the effective area to muon neutrinos) at the characteristic declinations of the six blazars considered here, to that of the IceCube HESE analysis, averaged

¹ The paper was released before the third PeV event, IC 35 (“Big Bird”), was made public. A search for possible blazar associations with this event is in preparation by the TANAMI Collaboration.

Table 1. Basic data on the six blazars studied in this analysis.

Source	Cat. Name	RA [°]	Dec [°]	Class	z	F_γ [GeV cm ⁻² s ⁻¹]	N_{ν_e}	IC
0235–618	PKS 0235–618	39.2218	−61.6043	Q	0.47 ^a	$(6.2^{+3.1}_{-3.1}) \times 10^{-8}$	$0.19^{+0.04}_{-0.04}$	20, 7
0302–623	PKS 0302–623	45.9610	−62.1904	Q	1.35 ^a	$(2.1^{+0.4}_{-0.4}) \times 10^{-8}$	$0.06^{+0.01}_{-0.01}$	20
0308–611	PKS 0308–611	47.4838	−60.9775	Q	1.48 ^a	$(4.7^{+1.8}_{-1.8}) \times 10^{-8}$	$0.14^{+0.05}_{-0.05}$	20
1653–329	Swift J1656.3–3302	254.0699	−33.0369	Q	2.40 ^b	$(2.8^{+0.3}_{-0.3}) \times 10^{-7}$	$0.86^{+0.10}_{-0.10}$	14, 2, 25
1714–336	TXS 1714–336	259.4001	−33.7024	B/Q	?	$(1.5^{+0.3}_{-0.4}) \times 10^{-7}$	$0.46^{+0.10}_{-0.12}$	14, 2, 25
1759–396	MRC 1759–396	270.6778	−39.6689	Q	1.32 ^c	$(7.5^{+1.9}_{-1.9}) \times 10^{-8}$	$0.23^{+0.50}_{-0.40}$	14, 2, 15, 25

Notes. Columns: (1) IAU B1950 name; (2) Common catalog name; (3), (4) J 2000 coordinates; (5) Classification: Q – Flat Spectrum Radio Quasar, B – BL Lac object; (6) Redshift: ^(a) Healey et al. (2008); ^(b) Cutri et al. (2003); ^(c) Massaro et al. (2009); (7) Total high-energy photon flux from Krauß et al. (2014); (8) Estimated number N_{ν_e} of ν_e events in the IceCube 662-day analysis (IceCube Collaboration 2013); (9) IC gives the IceCube event IDs from Aartsen et al. (2014) with which the blazars are positionally consistent within the angular error range from IceCube Collaboration (2013).

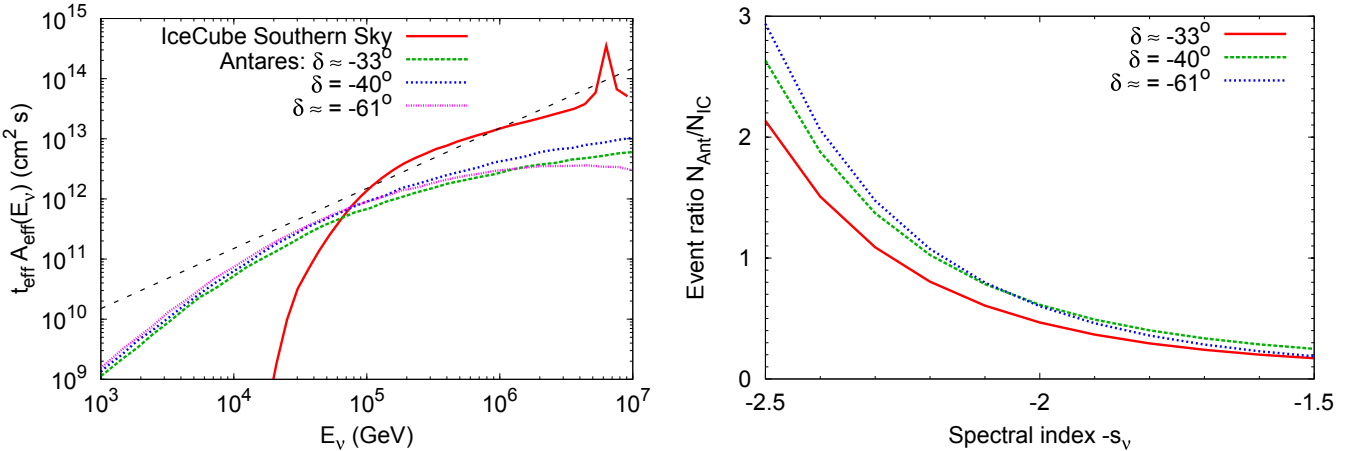


Fig. 1. Left: relative exposures of the ANTARES CLS (Adrián-Martínez et al. 2012) to a flavour-uniform neutrino flux from the characteristic declinations of the six candidate blazars, and the southern-sky-average of the IceCube HESE analysis (Aartsen et al. 2014) (exposures from IceCube Collaboration 2013). The black dashed line, included for reference, is proportional to E_ν . Right: expected number of ANTARES events per detected IceCube event for power-law spectra (Eq. (1)) as a function of the neutrino spectral index $-s_\nu$, calculated using the relative exposures.

over the southern hemisphere (IceCube Collaboration 2013; now updated to 998 days by Aartsen et al. 2014, averaged over all three neutrino flavours). It can be seen that below approximately 100 TeV, ANTARES has a greater sensitivity to a neutrino flux from the six blazars at the given southern declinations than the recent IceCube HESE analysis.

The predictions for the number of IceCube-detected PeV neutrino events by Krauß et al. (2014) were based on equating the neutrino flux at 1 PeV to the integrated photon flux between 1 keV and 10 GeV. While the expected neutrino-flux shape is highly model-dependent (as was discussed in Sect. 2), the prediction that the total neutrino energy flux F_ν (GeV cm⁻² s⁻¹) is approximately equal to the total high-energy photon flux F_γ is relatively robust, at least when attributing this emission to a 100% hadronic origin. The black-dashed line in Fig. 1 is proportional to neutrino energy E_ν and normalised to the IceCube exposure at 1 PeV, i.e., it is a line of equal sensitivity to a neutrino flux F_ν . For constant F_ν , it is clear that the IceCube HESE analysis is most sensitive to a flux at a few hundred TeV, while the ANTARES CLS is most sensitive near 30 TeV.

The range of potential neutrino spectra, $\Phi_\nu(E_\nu)$ (dN_ν/dE_ν), are characterised by generic power-law spectra with spectral index $-s_\nu$:

$$\Phi_\nu(E_\nu) = \Phi_0 \left(\frac{E_\nu}{1 \text{ GeV}} \right)^{-s_\nu} [\text{GeV}^{-1} \text{ cm}^{-2} \text{ s}^{-1}]. \quad (1)$$

The relative numbers of events expected to be observed by ANTARES compared to IceCube for such spectra are shown in Fig. 1 (right). The required energy in such fluxes to produce a single detectable event in ANTARES is calculated in Appendix A, and plotted in Fig. 2. In the range $-2.5 < -s_\nu < -1.5$, it is comparable with the total blazar photon flux calculated by Krauß et al. (2014) (see Table 1).

Having established a wide range of plausible neutrino flux scenarios, and the sensitivity of the ANTARES CLS to neutrino fluxes over a broad range of energies, we therefore perform the standard ANTARES CLS for an excess of neutrino emission from the six candidate blazars.

4. Results and discussion

The results of the ANTARES analysis of the six blazars are given in Table 2. For four of the six targets, no source-like neutrinos were identified ($N_{\text{sig}} = 0$), allowing relatively strong upper limits to be placed on an E_ν^{-2} flux. Blazars 1653–329 and 1714–336 were each fitted as having approximately one nearby signal-like event, with N_{sig} of 1.1 and 0.9 respectively². This observation is well within the expected background fluctuations, however,

² The maximum-likelihood procedure estimates N_{sig} as a continuous variable, as discussed in Sect. 3.

Table 2. ANTARES point-source analysis results.

Source	N_{sig}	p	Limit	$N_{\nu,\text{IC}} = 1, 2, 3, 4$			
0235–618	0	1	1.3	−2.4	−2.1	−2.0	−1.9
0302–623	0	1	1.3	−2.4	−2.1	−2.0	−1.9
0308–611	0	1	1.3	−2.4	−2.1	−2.0	−1.9
1653–329	1.1	0.10	2.9	<−2.5	−2.5	−2.3	−2.2
1714–336	0.9	0.04	3.5	<−2.5	−2.5	−2.3	−2.2
1759–396	0	1	1.4	−2.4	−2.1	−2.0	−1.8

Notes. Columns: (1) IAU B 1950 name; (2) number of fitted signal events; (3) pre-trial p -value; (4) 90% upper limit ($10^{-8} \text{ GeV}^{-1} \text{ cm}^{-2} \text{ s}^{-1}$) on Φ_0 for $-s_\nu = -2.0$; (5): minimum spectral indices $-s_\nu$ consistent at 90% C.L. with $N_{\nu,\text{IC}} = 1\dots 4$ associated IceCube events. Limits assume a flavour-uniform flux.

with pre-trial p -values (probability of the likelihood procedure fitting a stronger signal flux to background-only data) of 0.10 and 0.04, respectively³. Nonetheless, it must be noted that these two blazars have the highest predicted neutrino fluxes, and that from Fig. 1 (right), neutrino fluxes with spectral indices between −2.5 and −2.3 producing one IceCube event would be expected to produce between one and two ANTARES events. Therefore, when the calculation of Krauß et al. (2014) is extended to include power-law neutrino spectra, the result of the analysis is consistent with the sample blazars being neutrino sources with fluxes in proportion to their observed high-energy photon flux (F_γ in Table 1), even if the result is also consistent with background.

Limits at a 90% confidence level (C.L.), Φ_ν^{90} , on the spectra from Eq. (1) are generated from the ANTARES observations as a function of s_ν over the approximate predicted range (between 1.5 and 2.5), using the method of Neyman (1937). All are upper limits and are given in Fig. 3 (left). The confidence level is given at 100 TeV, because it is both the approximate energy at which the ANTARES and IceCube analyses have equal exposures and where the flux limit is least sensitive to s_ν .

The flux limits correspond to a maximum expected number $N_{\nu,\text{IC}}^{90}$ of events observed by IceCube; where this number is less than the observed number of events, a blazar origin can be excluded at 90% C.L. This is shown in Fig. 3 (right). Any given number of IceCube events is therefore only consistent with a blazar origin for neutrino spectral indices flatter than certain value; minimum values of $-s_\nu$ are given for 1–4 events in Table 2 and should be compared to the possible associations in Table 1. For the IC 14 field for instance, the possibility that blazar 1759–396 could be responsible for three or more associated IceCube events is excluded at 90% confidence for neutrino spectra steeper than −2.1. For spectra steeper than −2.4, we can exclude that 1759–396 is responsible for any IceCube events. The limits for 1653–329 and 1714–336 are weaker because of a possible physical association with the two signal-like ANTARES events. Regardless of the association, we can rule out the possibility that the cluster IC 14, IC 2, and IC 25 arose from a single considered blazar with a spectrum steeper than −2.4. For the IC 20 grouping, the non-observation of any event from the three candidate blazars means that the $\delta \approx -61^\circ$ limit applies both to the individual blazars, and the group as a whole. Therefore, ANTARES observations can rule out a neutrino spectrum steeper than −2.2 as being responsible for both IC 20 and IC 7, and a neutrino spectrum steeper than −2.4 being responsible for only one of them. That is, if IC 20 does indeed originate

from the three associated TANAMI blazars, the neutrino spectral index must be flatter than −2.4.

5. Conclusion

We have tested the hypothesis of Krauß et al. (2014) that the first two PeV neutrino events observed by IceCube, IC 14 and IC 20, are of blazar origin, by performing a CLS for an excess muon neutrino flux from the six suggested blazars using six years of ANTARES data. We are not able to either confirm or rule out a blazar origin of these events, although constraints have been placed on the range of source spectra which could have produced them, particularly in the case of IC 20. These constraints assume that muon neutrinos constitute one third of the neutrino flux, and strengthen or weaken proportionally with this fraction. While approximately two ANTARES events were fitted as being more signal-like than background-like by the maximum-likelihood analysis, such a result is completely within the expected background fluctuations, with pre-trial p -values of 10% and 4% for the blazars in question (1653–329 and 1714–336). It is interesting to note that these two blazars were predicted by Krauß et al. (2014) to have the strongest neutrino flux, and that such a result is within expectations for the ANTARES event rate for an E_ν^{-2} to $E_\nu^{-2.3}$ neutrino spectrum given that IceCube observes two such events, and $E_\nu^{-2.3}$ to $E_\nu^{-2.5}$ for a single event of blazar origin. Given these considerations, the TANAMI candidate blazars should be included in all future analyses.

Acknowledgements. The authors would like to thank A. Kappes for helpful discussions regarding the IceCube analysis. The ANTARES authors acknowledge the financial support of the funding agencies: Centre National de la Recherche Scientifique (CNRS), Commissariat à l'énergie atomique et aux énergies alternatives (CEA), Commission Européenne (FEDER fund and Marie Curie Program), Région Alsace (contrat CPER), Région Provence-Alpes-Côte d'Azur, Département du Var and Ville de La Seyne-sur-Mer, France; Bundesministerium für Bildung und Forschung (BMBF), Germany; Istituto Nazionale di Fisica Nucleare (INFN), Italy; Stichting voor Fundamenteel Onderzoek der Materie (FOM), Nederlandse organisatie voor Wetenschappelijk Onderzoek (NWO), the Netherlands; Council of the President of the Russian Federation for young scientists and leading scientific schools supporting grants, Russia; National Authority for Scientific Research (ANCS), Romania; Ministerio de Ciencia e Innovación (MICINN), Prometeo de Generalitat Valenciana and MultiDark, Spain; Agence de l'Oriental and CNRST, Morocco. We also acknowledge the technical support of Ifremer, AIM and Foselev Marine for the sea operation and the CC-IN2P3 for the computing facilities. The TANAMI authors acknowledge support and partial funding by the Deutsche Forschungsgemeinschaft grant WI 1860-10/1 (TANAMI) and GRK 1147, Deutsches Zentrum für Luft- und Raumfahrt grant 50 OR 1311/50 OR 1303/50 OR 1401, the Spanish MINECO project AYA2012-38491-C02-01, the Generalitat Valenciana project PROMETEOII/2014/057, the COST MP0905 action “Black Holes in a Violent Universe” and the Helmholtz Alliance for Astroparticle Physics (HAP).

References

- Aartsen, M. G., Abbasi, R., Abdou, Y., et al. 2013, *Phys. Rev. Lett.*, **111**, 021103
- Aartsen, M. G., Ackermann, M., Adams, J., et al. 2014, *Phys. Rev. Lett.*, **113**, 101101
- Aartsen, M. G., Ackermann, M., Adams, J., et al. 2015, *Phys. Rev. Lett.*, **91**, 022001
- Adrián-Martínez, S., Samarai, I. A., Albert, A., et al. 2012, *ApJ*, **760**, 53
- Adrián-Martínez, S., Albert, A., André, M., et al. 2014a, *ApJ*, **786**, L5
- Adrián-Martínez, S., Albert, A., André, M., et al. 2014b, *JCAP*, **11**, 017
- Ageron, M., Aguilar, J. A., Al Samarai, I., et al. 2011, *Nucl. Instr. Meth. Phys. Res. A*, **656**, 11
- Anchordoqui, L. A. 2015, *Phys. Rev. D*, **91**, 027301
- Atoyan, A., & Dermer, C. D. 2001, *Phys. Rev. Lett.*, **87**, 221102
- Beacom, J. F., Bell, N. F., Hooper, D., Pakvasa, S., & Weiler, T. J. 2003, *Phys. Rev. D*, **68**, 093005
- Becker Tjus, J., Eichmann, B., Halzen, F., Kheirandish, A., & Saba, S. M. 2014, *Phys. Rev. D*, **89**, 123005

³ The correct penalty factor for multiple trials is 61, including the six blazars considered here, and 55 trials from other analyses using the CLS (Adrián-Martínez et al. 2014a,b).

- Berezinskii, V. S., & Smirnov, A. I. 1975, *Ap&SS*, **32**, 461
 Cutri, R. M., Skrutskie, M. F., van Dyk, S., et al. 2003, VizieR Online Data Catalog: II/246
 Dermer, C. D., Murase, K., & Inoue, Y. 2014, *J. High Energy Astrophys.*, **3**, 29
 Healey, S. E., Romani, R. W., Cotter, G., et al. 2008, *ApJS*, **175**, 97
 Hillas, A. M. 1984, *ARA&A*, **22**, 425
 IceCube Collaboration 2013, *Science*, **342**, 1242856
 IceCube Collaboration, Aartsen, M. G., Ackermann, M., et al. 2015, *Phys. Rev. Lett.*, submitted [[arXiv:1502.03376](https://arxiv.org/abs/1502.03376)]
 Kelner, S. R., Aharonian, F. A., & Bugayov, V. V. 2006, *Phys. Rev. D*, **74**, 034018
 Kistler, M. D., Stanev, T., & Yüksel, H. 2014, *Phys. Rev. D*, **90**, 123006
 Krauß, F., Kadler, M., Mannheim, K., et al. 2014, *A&A*, **566**, L7
 Mannheim, K. 1995, *Astropart. Phys.*, **3**, 295
 Massaro, E., Giommi, P., Leto, C., et al. 2009, *A&A*, **495**, 691
 Neyman, J. 1937, *Roy. Soc. London Phil. Trans. Ser. A*, **236**, 333
 Padovani, P., & Resconi, E. 2014, *MNRAS*, **443**, 474
 Razzaque, S. 2013, *Phys. Rev. D*, **88**, 081302
 Stecker, F. W., & Salamon, M. H. 1996, *Space Sci. Rev.*, **75**, 341
 Szabo, A. P., & Protheroe, R. J. 1994, *Astropart. Phys.*, **2**, 375
 Véron-Cetty, M.-P., & Véron, P. 2006, *A&A*, **455**, 773
 Waxman, E., & Bahcall, J. 1999, *Phys. Rev. D*, **59**, 023002

- ¹ Institut d'Investigació per a la Gestió Integrada de les Zones Costaneres (IGIC) – Universitat Politècnica de València. C/ Paranimf 1, 46730 Gandia, Spain
² GRPHE – Université de Haute Alsace – Institut Universitaire de Technologie de Colmar, 34 rue du Grillenbreit, BP 50568, 68008 Colmar, France
³ Technical University of Catalonia, Laboratory of Applied Bioacoustics, Rambla Exposició, 08800 Vilanova i la Geltrú, Barcelona, Spain
⁴ INFN–Sezione di Genova, via Dodecaneso 33, 16146 Genova, Italy
⁵ Friedrich-Alexander-Universität Erlangen-Nürnberg, Erlangen Centre for Astroparticle Physics, Erwin-Rommel-Str. 1, 91058 Erlangen, Germany
⁶ CPPM, Aix-Marseille Université, CNRS/IN2P3, 13009 Marseille, France
⁷ APC, Université Paris Diderot, CNRS/IN2P3, CEA/IRFU, Observatoire de Paris, Sorbonne Paris Cité, 75205 Paris, France
⁸ IFIC – Instituto de Física Corpuscular, Edificios Investigación de Paterna, CSIC – Universitat de València, Apdo. de Correos 22085, 46071 Valencia, Spain
⁹ LAM – Laboratoire d'Astrophysique de Marseille, Pôle de l'Étoile Site de Château-Gombert, rue Frédéric Joliot-Curie 38, 13388 Marseille Cedex 13, France
¹⁰ INFN–Sezione di Bologna, viale Berti-Pichat 6/2, 40127 Bologna, Italy
¹¹ Dipartimento di Fisica e Astronomia dell'Università, Viale Berti-Pichat 6/2, 40127 Bologna, Italy
¹² Nikhef, Science Park, 1098 XG Amsterdam, The Netherlands
¹³ Huygens-Kamerlingh Onnes Laboratorium, Universiteit Leiden, 2300 RA Leiden, The Netherlands
¹⁴ Universiteit van Amsterdam, Instituut voor Hoge-Energie Fysica, Science Park 105, 1098 XG Amsterdam, The Netherlands
¹⁵ INFN–Sezione di Roma, Ple Aldo Moro 2, 00185 Roma, Italy
¹⁶ Dipartimento di Fisica dell'Università La Sapienza, P.le Aldo Moro 2, 00185 Roma, Italy
¹⁷ Institute for Space Science, 077125 Bucharest, Măgurele, Romania
¹⁸ INFN–Sezione di Bari, via E. Orabona 4, 70126 Bari, Italy
¹⁹ INFN–Sezione di Napoli, via Cintia 80126 Napoli, Italy
²⁰ Dipartimento di Fisica dell'Università Federico II di Napoli, via Cintia 80126 Napoli, Italy
²¹ Mediterranean Institute of Oceanography (MIO), Aix-Marseille University, 13288 Marseille, Cedex 9, France
²² Université du Sud Toulon-Var, CNRS-INSU/IRD UM 110, 83957 La Garde Cedex, France
²³ Géoazur, Université Nice Sophia-Antipolis, CNRS/INSU, IRD, Observatoire de la Côte d'Azur, Sophia Antipolis, France
²⁴ INFN–Laboratori Nazionali del Sud (LNS), via S. Sofia 62, 95123 Catania, Italy
²⁵ Univ. Paris-Sud , 91405 Orsay Cedex, France
²⁶ Kernfysisch Versneller Instituut (KVI), University of Groningen, Zernikelaan 25, 9747 AA Groningen, The Netherlands
²⁷ Laboratoire de Physique Corpusculaire, Clermont Université, Université Blaise Pascal, CNRS/IN2P3, BP 10448, 63000 Clermont-Ferrand, France
²⁸ INFN–Sezione di Catania, viale Andrea Doria 6, 95125 Catania, Italy
²⁹ Royal Netherlands Institute for Sea Research (NIOZ), Landsdiep 4, 1797 SZ 't Horntje (Texel), The Netherlands
³⁰ Universiteit Utrecht, Faculteit Betawetenschappen, Princetonplein 5, 3584 CC Utrecht, The Netherlands
³¹ Dr. Remeis-Sternwarte and ECAP, Universität Erlangen-Nürnberg, Sternwartstr. 7, 96049 Bamberg, Germany
³² Dipartimento di Fisica ed Astronomia dell'Università, viale Andrea Doria 6, 95125 Catania, Italy
³³ Direction des Sciences de la Matière – Institut de recherche sur les lois fondamentales de l'Univers – Service de Physique des Particules, CEA Saclay, 91191 Gif-sur-Yvette Cedex, France
³⁴ IPHC-Institut Pluridisciplinaire Hubert Curien – Université de Strasbourg et CNRS/IN2P3, 23 rue du Loess, BP 28, 67037 Strasbourg Cedex 2, France
³⁵ ITEP – Institute for Theoretical and Experimental Physics, B. Cheremushkinskaya 25, 117218 Moscow, Russia
³⁶ Dipartimento di Fisica dell'Università, via Dodecaneso 33, 16146 Genova, Italy
³⁷ University Mohammed I, Laboratory of Physics of Matter and Radiations, BP 717, 6000 Oujda, Morocco
³⁸ Institut für Theoretische Physik und Astrophysik, Universität Würzburg, Emil-Fischer-Str. 31, 97074 Würzburg, Germany
³⁹ NASA, Goddard Space Flight Center, Greenbelt, MD 20771, USA
⁴⁰ University of Maryland, Baltimore County, Baltimore, MD 21250, USA
⁴¹ Catholic University of America, Washington, DC 20064, USA
⁴² Max-Planck-Institut für Radioastronomie, Auf dem Hügel 69, 53121 Bonn, Germany
⁴³ Departament d'Astronomia i Astrofísica, Universitat de València, C/ Dr. Moliner 50, 46100 Burjassot, València, Spain
⁴⁴ Observatori Astronòmic, Universitat de València, C/ Catedràtic José Beltrán No. 2, 46980 Paterna, València, Spain
⁴⁵ Departamento de Astronomía, Universidad de Concepción, Casilla 160, Chile
⁴⁶ CSIRO Astronomy and Space Science, ATNF, PO Box 76 Epping, NSW 1710, Australia
⁴⁷ Max-Planck-Institut für extraterrestrische Physik, Giessenbachstraße 1, 85741 Garching, Germany
⁴⁸ Bundesamt für Kartographie und Geodäsie, 93444 Bad Kötzting, Germany
⁴⁹ CSIRO Astronomy and Space Science, Canberra Deep Space Communications Complex, PO Box 1035, Tuggeranong, ACT 2901, Australia
⁵⁰ School of Mathematics & Physics, University of Tasmania, Private Bag 37, Hobart, Tasmania 7001, Australia
⁵¹ Hartebeesthoek Radio Astronomy Observatory, 1740 Krugersdorp, South Africa

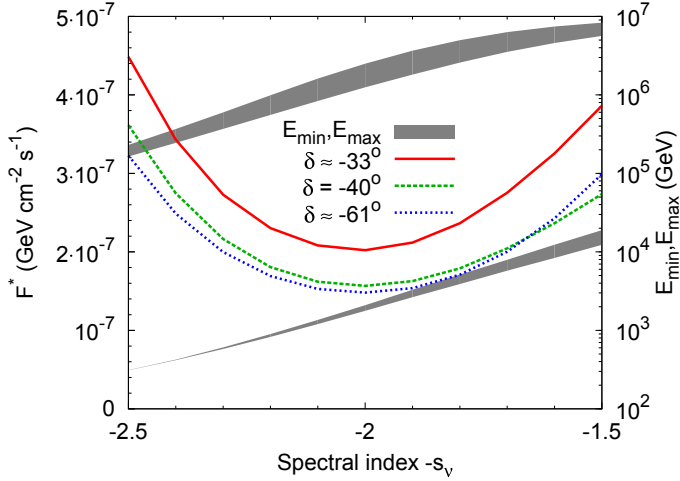


Fig. 2. Neutrino flux F_ν^* required to produce one neutrino event in ANTARES as a function of spectral index s_ν (Eq. (A.3)). The corresponding energy ranges of integration E_{\min} and E_{\max} (Eq. (A.2)) are shown as lower and upper shaded regions respectively: the shading covers the variation due to declination.

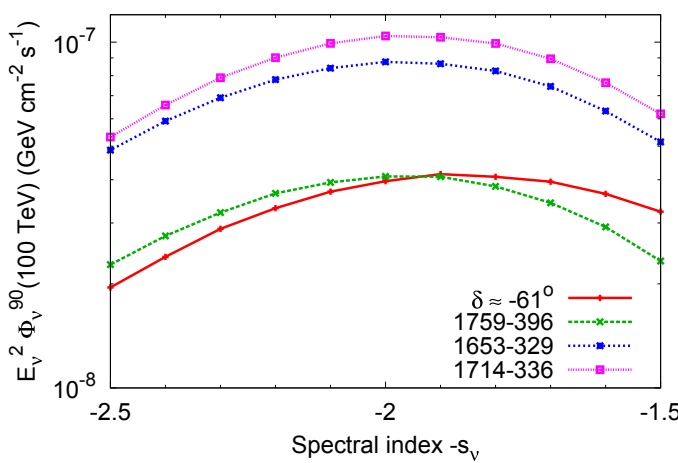


Fig. 3. *Left:* ANTARES 90% confidence limits on a flavour-uniform neutrino flux ($\Phi_\nu \equiv \Phi_{\nu_e} + \Phi_{\nu_\mu} + \Phi_{\nu_\tau} = 3\Phi_{\nu_\mu}$) from the six blazars as a function of spectral index s_ν (Eq. (1)). *Right:* corresponding limits on the expected number of IceCube events of blazar origin, using the exposures shown in Fig. 1 and the limiting fluxes. Since the limits from 0235–618, 0302–623, and 0308–611 are almost identical, and since no events were observed, the limits also apply to the summed flux from all three of these blazars, and hence only one line is shown, and is labelled “IC 20 TANAMI blazars”.

Appendix A: Calculation of neutrino energy flux

For each spectral index $-s_\nu$ and source declination δ , the required neutrino flux $\Phi_\nu^*(E_\nu, \delta)$ expected to produce a single ANTARES event can be found from the expression

$$\int_0^\infty t_{\text{eff}} A_{\text{eff}}(E_\nu) \Phi_\nu^*(E_\nu, \delta) dE_\nu = 1, \quad (\text{A.1})$$

where $A_{\text{eff}}(E_\nu, \delta)$ and t_{eff} are respectively the ANTARES effective area and the observation time. While the total energy in such a flux is infinite, the energy over the sensitive range of ANTARES can be calculated by defining characteristic energies $E_{\min}(\delta, s_\nu)$ and $E_{\max}(\delta, s_\nu)$ such that:

$$\int_{E_{\min}}^{E_{\max}} t_{\text{eff}} A_{\text{eff}}(E_\nu, \delta) \Phi_\nu^*(E_\nu, \delta) dE_\nu = 0.9, \quad (\text{A.2})$$

with 0.05 below E_{\min} and 0.05 above E_{\max} . The total neutrino energy flux $F_\nu^*(\delta, s_\nu)$ in the range $E_{\min} \leq E_\nu \leq E_{\max}$ required to produce one event can then be calculated from $\Phi_\nu^*(E_\nu, \delta)$ as:

$$F_\nu^*(\delta, s_\nu) = \frac{1}{0.9} \int_{E_{\min}}^{E_{\max}} \Phi_\nu^*(E_\nu, \delta) E_\nu dE_\nu \left[\text{GeV cm}^{-2} \text{s}^{-1} \right]. \quad (\text{A.3})$$

In Fig. 2 $F_\nu^*(\delta, s_\nu)$ is plotted along with E_{\min} and E_{\max} .